

## Introduction

Creating the Chandra Source Catalog (Evans et al, Poster 472.01) required adjustment of existing pipeline processing, adaptation of existing interactive analysis software for automated use, and development of entirely new algorithms. Data calibration was based on the existing pipeline, but more rigorous data cleaning was applied and the latest calibration data products were used. For source detection, a local background map was created including the effects of ACIS source readout streaks. The existing wavelet source detection algorithm was modified and a set of post-processing scripts used to correct the results. To analyse the source properties we ran the SAOTrace ray trace code for each source to generate a model point spread function, allowing us to find encircled energy correction factors and estimate source extent. Further algorithms were developed to characterize the spectral, spatial and temporal properties of the sources and to estimate the confidence intervals on count rates and fluxes. Finally, sources detected in multiple observations were matched, and best estimates of their merged properties derived. In this paper we present an overview of the algorithms used. More detailed treatment of some of the newly developed algorithms are presented in companion posters. For details of the software and processing, see J. Evans et al, Poster 472.06; for a description of the user interface which allows access to the catalog, see Bonaventura et al, Poster 472.02.

## Data calibration

We use the standard CIAO (Fruscione et al, 2006, SPIE 6270,60) tools to create an observation-specific bad pixel file with the latest calibrations. This file is used to filter the data and ensures that events from hot pixels and cosmic-ray afterglow effects are not included; the calculated exposure depth is adjusted to account for the excluded pixels. Initial event processing and filtering is the same as in the standard pipeline (I. Evans et al, 2006, SPIE 6270, 59). The positions of the photons are transformed from the detector to the sky using time-tagged RA, Dec and spacecraft roll derived from aspect camera data. Event instrumental energy (PHA) values are adjusted for instrument gain as a function of detector position and epoch and are corrected for charge transfer inefficiency.

## Flare removal

We further filter the data to remove background flares, improving our sensitivity to faint diffuse emission.

Bright sources are excluded from the data and a light curve is constructed using the method of Gregory and Loredo (1992, ApJ 398, 146). The minimum count rate in this light curve is determined, and time ranges with more than 10 times this rate are excluded from the data.

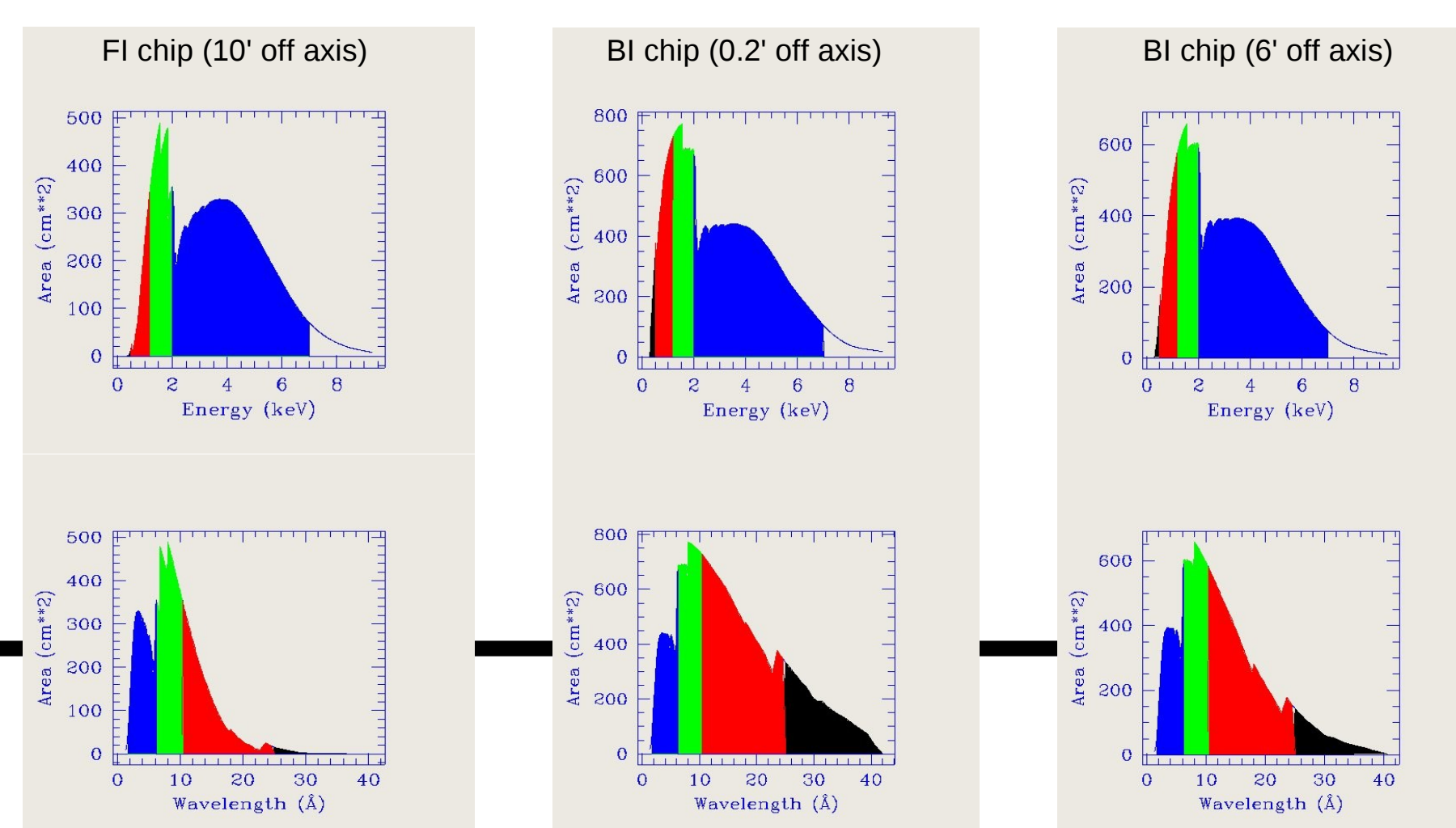
## Source Detection - Wavelet analysis

Source candidates are generated by correlation of the energy-band-filtered images with Mexican Hat wavelets on different spatial scales and then combining the results across scales and energy bands to create a single source list. Position errors are determined as a function of net counts and off axis angle, using a calibration from the ChaMP catalog (Kim et al, 2004, ApJS 150,19)

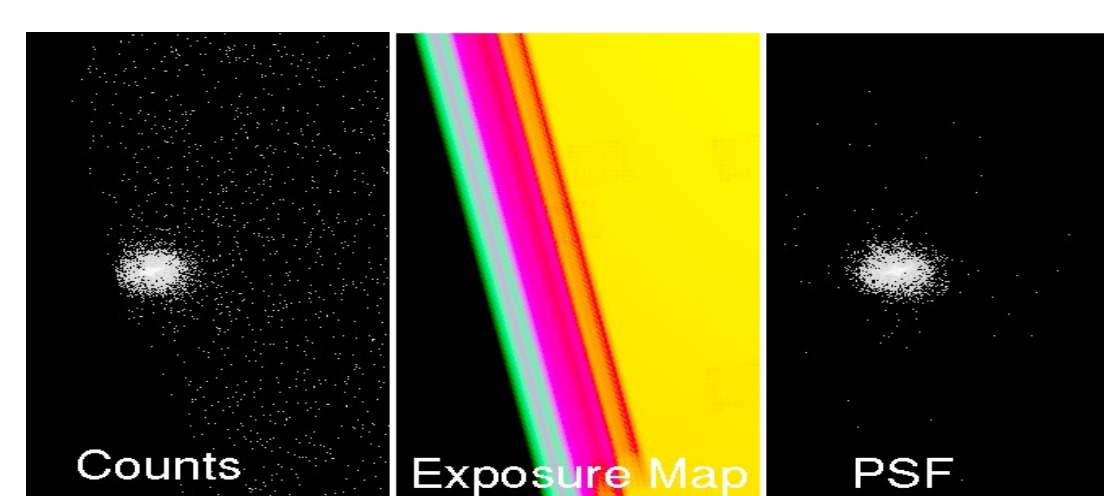
## Source Detection - global background

For each observation, a background map is determined using the algorithm discussed by McCollough et al (Poster 472.10). The image is divided into coarsely blocked regions and a mean count rate determined for each region. This low frequency background map is insufficient for ACIS data, which contain streaks due to photons arriving while the chip is being read out. A streak map added to the low frequency background improves the detection of faint sources in regions affected by the streaks.

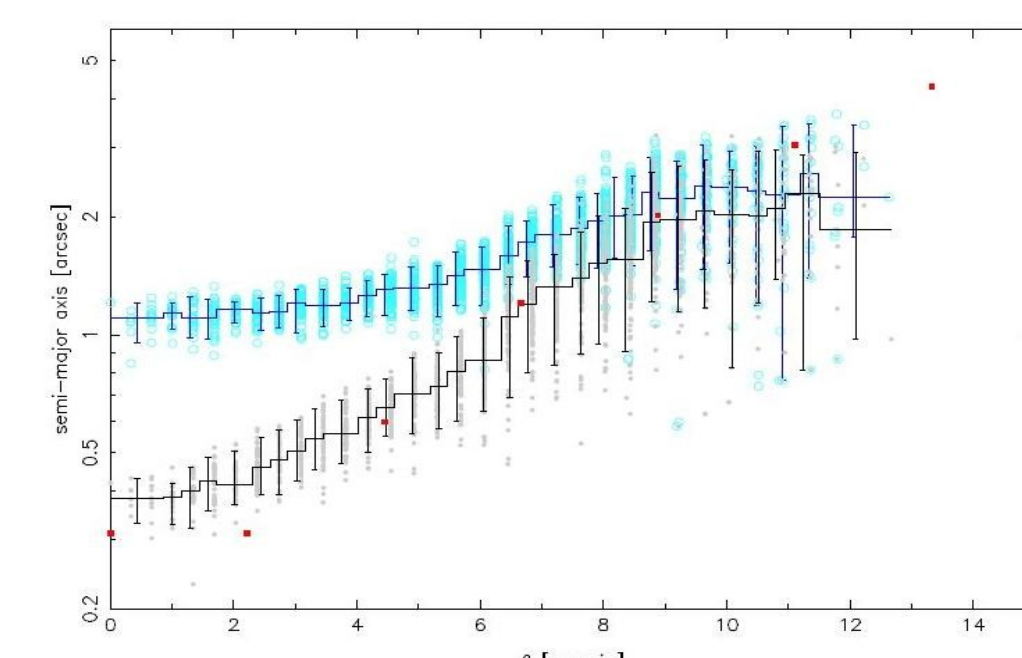
The background map is used in our wavelet-based detection algorithm to determine source existence, significance and source positions. However, it is not used to determine source and background count rates and fluxes.



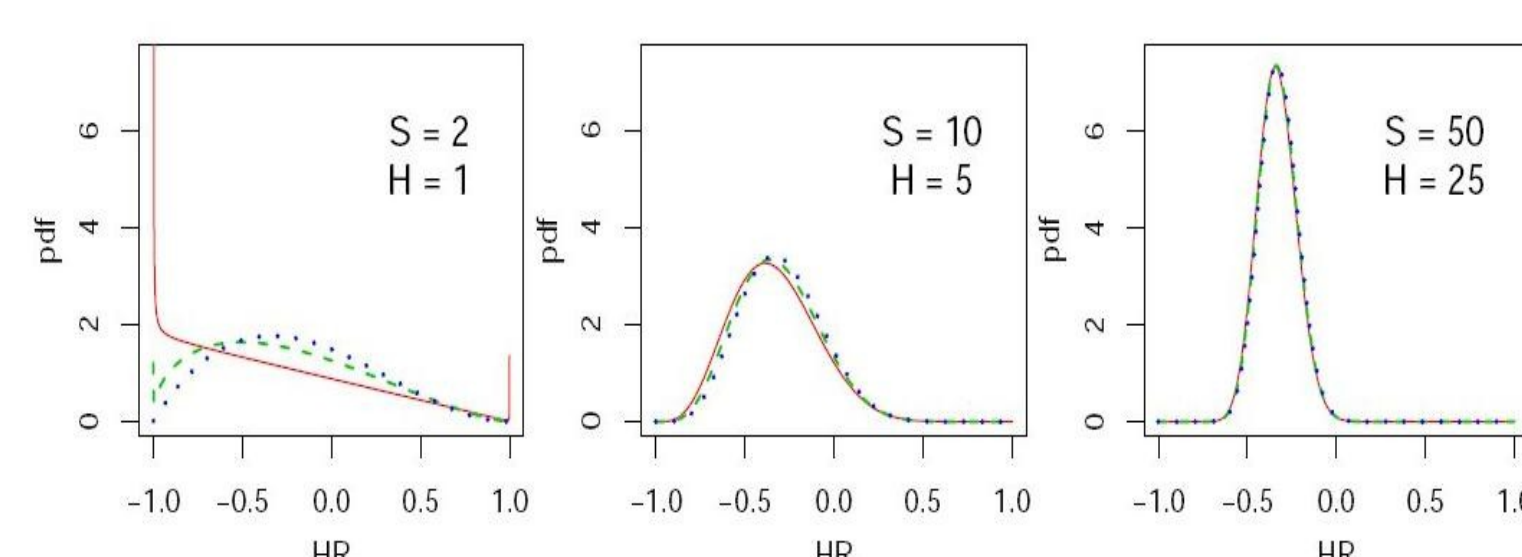
Sample Chandra/ACIS sensitivity curves, showing the energy bands used in the catalog. The energy bands are 0.2-0.5 keV (black), 0.5-1.0 keV (red), 1.0-2.0 keV (green) and 2.0-7.0 keV (blue). Upper panels: effective collecting area versus energy in keV; lower panels, same versus wavelength in Å. ACIS has 10 chips, of two different types; BI (back illuminated) chips have higher low-energy sensitivity than the FI (front illuminated) chips.



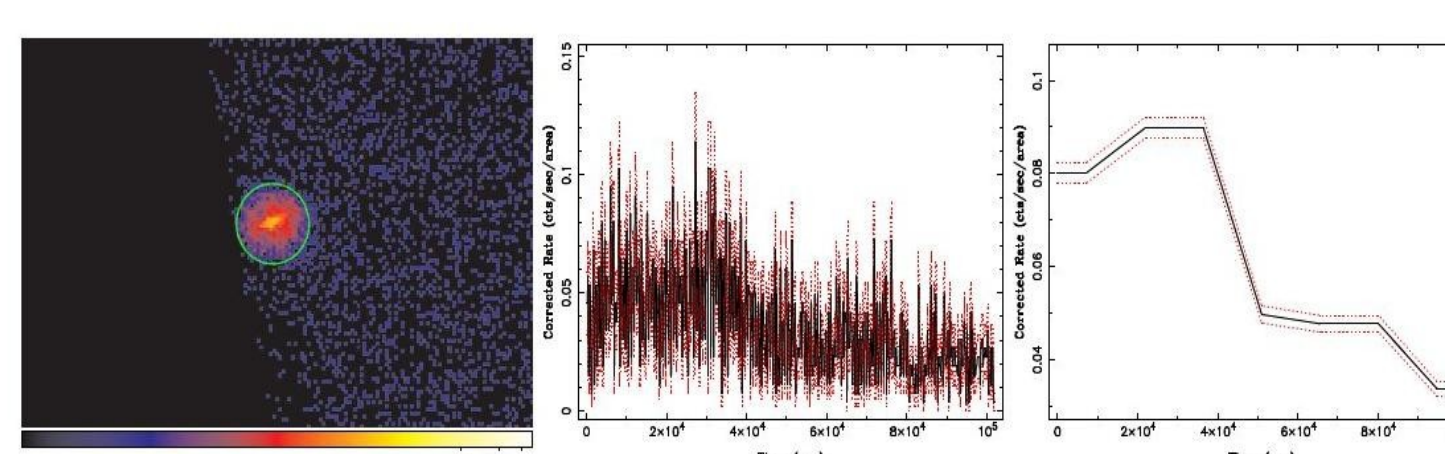
Source image cutout (left); corresponding exposure map giving the spatial variation of the product of pixel sensitivity and exposure time (center); model point spread function from ray trace (right).



Calibration of MHO algorithm (Houck et al, in prep) versus source off-axis angle. Points are simulated sources with 130 counts, error bars are 90-percent-confidence MHO-derived estimates. The blue sources are 2" extended disks, grey sources are points, both convolved with Chandra PSF. The red squares show the expected true size of the Chandra PSF (40% encircled energy). It may be seen that, with these assumptions, point and extended sources can be distinguished out to 5 arcmin off axis.



Given a fixed number of counts S and H in the soft and hard bands, and 10 background counts, the Bayesian estimate of the hardness ratio (H-S)/(H+S) shows an increasingly Gaussian distribution for increasing counts. (from Park et al, 2006, ApJ 652, 610).



Light curve dither correction. Left: source region near chip edge. Center: Light curve without correction. Right: with correction. See Nowak et al (poster 472.11).

## Source Merging and Characterization

The merging of sources seen in multiple observations is discussed by Hain et al (Poster 472.07). The intent of the merged source catalog is to include each detected astrophysical object exactly once, and give a best estimate of the object's properties assuming that they are not time-variable. We do not co-add the data prior to detection, so faint deep field sources are not found in this release of the catalog. We intend to perform co-added detections in our second release of the catalog.

The overall statistical characterization of the catalog has been carried out using realistic simulations processed through the operational catalog pipelines (Primini et al, poster 472.05).

## Source Properties

For each source, count rates were determined using aperture photometry and a Bayesian confidence interval error calculation (see Kashyap et al, poster 472.09 for details). Where possible, we also determine spatial extent using a wavelet based method, 'Mexican-hat optimization' (MHO: J. Houck et al, in preparation).

Like all X-ray telescopes, Chandra has a PSF which increases rapidly in size with off-axis angle, so a PSF size estimate is important for source interpretation. The SAOTrace ray trace program is used to generate a PSF image at the location of the source. Using elliptical 'Mexican-hat' wavelet functions, the wavelet transforms of both the PSF image and the actual image cutout are computed and used to estimate effective Gaussian sizes for both the PSF and the source. Confidence intervals on the sizes were calibrated as a function of total counts using simulations, and scale approximately as  $1/\sqrt{n}$ .

A deconvolved size is also derived by convolving a circular Gaussian with the PSF image and finding the best fit radius to match the observed sources. Of course, the confidence intervals on this size are consistent with zero intrinsic extent for the majority of sources in the catalog.

The PSF is also used to calculate a region containing 90 percent of the observed flux of a point source at the given location. Count rates are given in this 90-percent ellipse as well as in a source region derived from the wavelet source detection.

See also the poster by Rots et al (472.03) for details on the source properties derived, Doe et al. (472.04) for the derivation of the spectral properties, and Nowak et al. (472.11) for the variability algorithms.

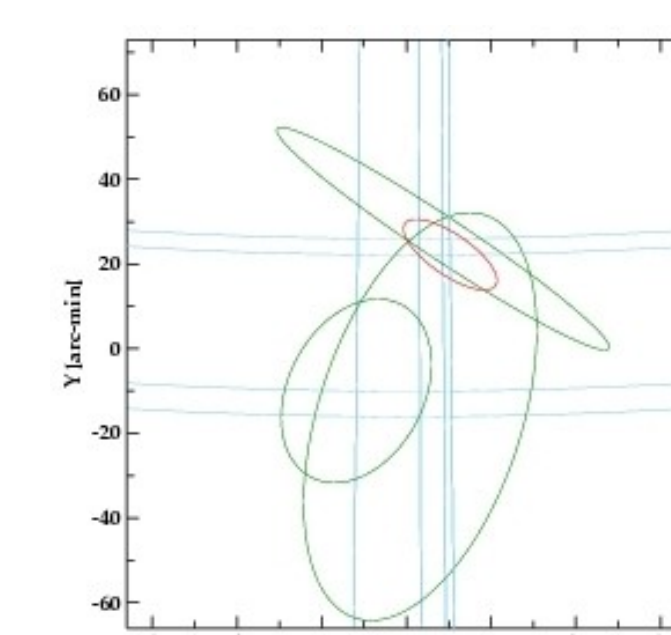
**Spectral analysis:** For each source in the catalog, the effective area (flux sensitivity curve as a function of energy) and redistribution matrix (line spread function) are computed and archived in standard ARF and RMF FITS files. Calibrations are applied for the observation epoch and are weighted over the detector area swept out by the source during the telescope dither pattern.

For sources with more than 150 net counts in 0.5-7.0 keV, power law and black body spectral models are fit using Sherpa (Doe et al, 2007, ADASS XVI, 543). Two-sided confidence intervals are given for fit parameters. For fainter sources, only 'hardness ratios' (broad band colors) are provided. These are calculated from the source fluxes in each band using the Bayesian estimators described by Park et al (2006, ApJ 652, 610).

**Variability analysis:** the algorithm of Gregory and Loredo, already applied to the background for flare removal, is now used to obtain a source light curve. The algorithm is adjusted to take exposure effects into account, so that true source variability can be determined even in the presence of a chip gap within the dither pattern. The G-L light curve weights multiple different time-binnings of the data with the log of their likelihoods, correcting for the fractional exposure in each time bin. However, spatial variations in the quantum efficiency are not taken into account.

For sources detected in more than one observation, the merged catalog combines position ellipse data using an 2-dimensional optimal weighting algorithm adapted by J. Davis from J.R. Orechovesky (1996, NPS MSc Thesis); the ellipse covariance matrices are combined with weightings proportional to their inverse uncertainties.

The figure below shows an extreme case, with significantly different error ellipses from three different observations (green) and the resulting best estimate position error ellipse (red).



## ACKNOWLEDGEMENTS

Support of the development of the Chandra Source Catalog is provided by the National Aeronautics and Space Administration through the Chandra X-ray Center, which is operated by the Smithsonian Astrophysical Observatory for and on behalf of the National Aeronautics and Space Administration under contract NAS8-03060